J.-Y. Yung and F. V. Lawrence, Jr†*

Predicting the Fatigue Life of Welds Under Combined Bending and Torsion

REFERENCE Yung, J. Y. and Lawrence, F. V., Jr, **Predicting the fatigue life of welds under combined bending and torsion,** *Biaxial and Multiaxial Fatigue*, EGF 3 (Edited by M. W. Brown and K. J. Miller), 1989, Mechanical Engineering Publications, London, pp. 53–69.

ABSTRACT Tube-to-plate weldments were fatigue tested under combined bending and torsion loadings. The initiation and early growth of cracks were restricted to the weld toe. Compressive residual stresses were measured at the weld toe using X-ray methods. Thermal stress relief lowered the weld-toe residual stresses and reduced the fatigue life. Two approaches were investigated to predict the fatigue crack initiation life.

The first approach used three different strain-based parameters: the maximum shearing strain amplitude, the Lohr–Ellison parameter, and the Kandil–Brown–Miller parameter. These parameters were combined with the Coffin–Manson equation to predict the fatigue crack initiation life under multiaxial, cyclic stresses. The required notch-root strains were calculated using an elastic–plastic finite element analysis.

The second approach employed the Basquin equation modified to estimate the fatigue life of welds for lives greater than 10^5 cycles. The worst-case-notch condition was assumed to be valid for both torsion and bending. The predicted fatigue lives were within a factor of three of the observed fatigue lives of the tube-to-plate weldments.

Notation

b	Fatigue strength exponent
c	Fatigue ductility exponent
E	Modulus of elasticity
k, s	Constants
K_{fmax}	Maximum fatigue notch factor
N_{I}	Cycles to crack initiation and early growth
N_{f}	Cycles to failure
S_{a}	Nominal stress amplitude
γ	Shear strain
γ^*	Maximum shear strain on a plane intersecting the free surface at 45 degrees
γ_{max}	Maximum shear strain
ε'_{f}	Fatigue ductility coefficient
ε_{n}	Strain normal to γ_{max} plane
ε^*_{n}	Strain normal to γ^* plane
ε	Normal strain

* Sundstrand Corporation, Rockford, IL 61125, USA.
† Department of Civil Engineering and Metallurgy, University of Illinois at Urbana-Champaign, Urbana, IL 61801, USA.

τ_a Shear stress amplitude
σ_a Local stress amplitude
σ'_f Fatigue strength coefficient
σ_{no} Mean stress normal to γ_{max} plane
σ^*_{no} Mean stress normal to γ^* plane
σ_r Residual stress

Superscripts
B Bending
E Equivalent stress
P Principal stress
T Torsion

The application of multiaxial fatigue concepts to weldments

Weldments are often subjected to multiaxial loading as are many notched, structural components: welded girders and shafts are common examples. Weldments differ from other notched structural components in at least two respects: welding usually induces high residual stresses at the fatigue crack initiation sites; and welds are irregular and, therefore, difficult notches to quantify.

Weld toes are frequently the sites of fatigue crack initiation and can be regarded as two-dimensional notches of infinite length. While the stresses and strains normal to the weld are greatly magnified at the weld-toe notch root and lead to fatigue failure, there is mounting evidence that stresses and strains parallel to the line of the notch root may also increase the severity of the problem, despite the fact that stresses and strains parallel to the toe have rather low stress concentration factors. Previous studies by Munse (**1**) suggested that shearing stresses reduce the fatigue life of weldments, and that better correlations between fatigue life test data and applied stress can be obtained using the principal stresses near the weld toe rather than the stresses and strains normal to the toe.

The object of this study was to apply recent ideas in multiaxial fatigue theory to tube-to-plate weldments subjected to bending and torsion loading. Most multiaxial fatigue theories attempt to predict multiaxial fatigue behavior using uniaxial fatigue data. Early studies correlated multiaxial fatigue data with the maxima of principal strain amplitude, shear strain amplitude, or octahedral strain amplitude. Recent work emphasizes the concept of a critical plane for crack initiation and growth. Lohr and Ellison (**2**) proposed the following relationship based on the maximum shear strain on planes intersecting the free surface and the strain normal to the crack plane

$$\gamma^* + k\varepsilon^*_n = \text{constant} \tag{1}$$

where

γ^* = the maximum shear strain amplitude on planes intersecting the free surface at 45 degrees which drives the crack through the thickness
ε_n^* = the strain amplitude normal to the γ^* plane
k = constant, 0.4 for three steels

Kandil, Brown, and Miller (**3**) proposed a relationship based on the maximum shear strain amplitude and the strain normal to the crack plane

$$\frac{\Delta\gamma_{max}}{2} + s\varepsilon_n = \text{constant} \tag{2}$$

where

$\gamma_{max}/2$ = the maximum shear strain amplitude
ε_n = the strain amplitude normal to the maximum shear plane
s = 1 when strain amplitude is used in the expression (4)

While neither of the above relationships includes the effects of mean stress, the influence of the mean stress normal to the shear plane (σ_{no}) can be incorporated by modifying the shear strain parameters (**5**)(**6**). Fash and Socie (**5**)(**6**) combined several of the above mentioned parameters and relationships with the well known Coffin–Manson equation, which describes strain controlled fatigue, and obtained the following expressions

$$\frac{\Delta\gamma_{max}}{2} = 1.3\frac{\sigma_f'}{E}(2N_f)^b + 1.5\varepsilon_f'(2N_f)^c \tag{3}$$

$$\gamma^* + 0.4\varepsilon_n^* + \frac{\sigma_{no}^*}{E} = 1.44\frac{\sigma_f'}{E}(2N_f)^b + 1.60\varepsilon_f'(2N_f)^c \tag{4}$$

$$\frac{\Delta\gamma_{max}}{2} + \varepsilon_n + \frac{\sigma_{no}}{E} = 1.65\frac{\sigma_f'}{E}(2N_f)^b + 1.75\varepsilon_f'(2N_f)^c \tag{5}$$

The fatigue crack initiation life of the 20 tube-to-plate weldments investigated were compared with fatigue crack initiation life estimates made using the three relationships above and an analysis based on the Basquin equation and the fatigue notch factor concept. While estimates of the fatigue crack propagation life could, in principle, have been obtained using the concept of the effective stress intensity factor, no such estimates were made in this study because of the complex nature of fatigue crack growth and the lack of a model for the stress intensity factor for the geometry of the test pieces used in this study.

Experimental methods and results

Tube-to-plate weldments having the geometry and dimensions shown in Fig. 1 were fabricated from 47.6 mm diameter seamless, cold-drawn steel tubing meeting the ASTM A519 standard and having a yield strength of 552 MPa and

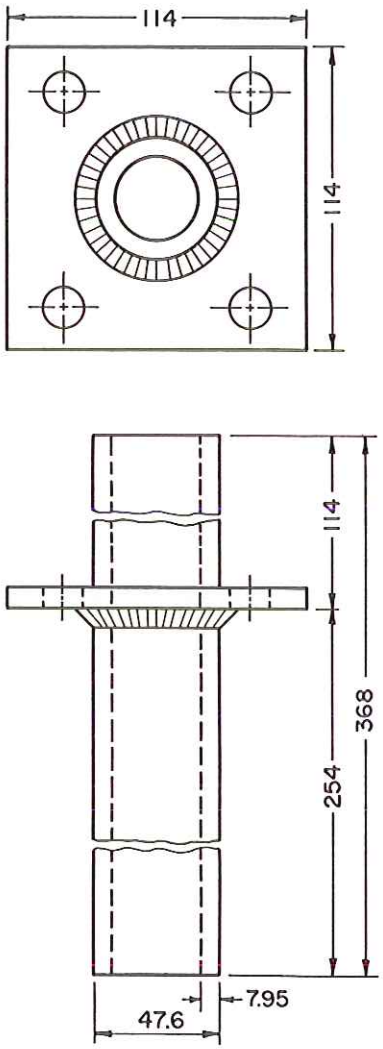

Fig 1 Specimen geometry of the tube-to-plate welds (units in mm). Fatigue cracks initiated at the weld toe formed by the tube outer surface and the weld metal

an ultimate strength of 700 MPa. Welding was carried out using an automatic gas–metal-arc process operated at 25 volts and 150 amperes with an argon–2% oxygen shielding gas. The solid, filler-metal wire had a diameter of 0.89 mm and met the AWS E70S standard. The weld size was approximately equal to the tube thickness. Both as-welded and stress-relieved (650°C for 4 hours) test pieces were prepared. Stress relief did not greatly alter the hardness of the weld region microstructures: see Fig. 2.

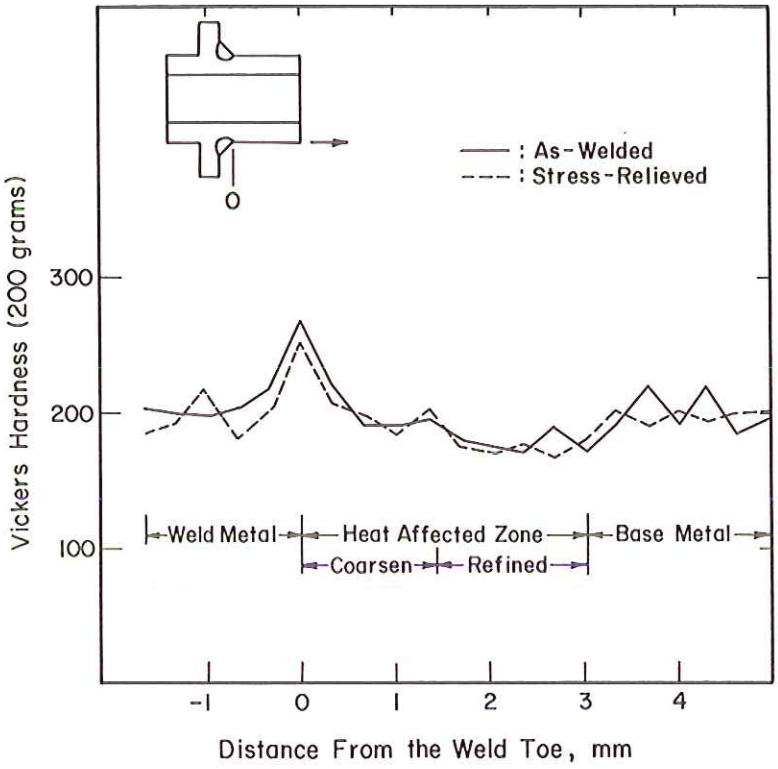

Fig 2 Results of Vickers pyramid hardness (200 grams load) surveys 0.15 mm below the outer surface of steel tubing. The locationof the hardness readings were measured from the weld toe along the surface of the tube. The positive direction is away from the weld toe

The axial and circumferential residual stresses which developed during welding were measured using X-ray diffraction methods. Residual stresses were measured at the weld toe and along a path away from the toe and down the axis of the tube. The variations of residual stress below the outer surface of the tube were measured by successively electropolishing material from the outer surface. The measured and calculated residual stresses are listed in Table 1. Figure 3 shows the variation of residual stress near the weld toe at the surface of the tube. The results of the residual stress measurements confirm that girth welds can have compressive residuals at their weld toes (7).

The test apparatus used was designed for the biaxial fatigue program of the Society of Automotive Engineers Fatigue Design and Evaluation Committee (5). As can be seen in Fig. 4, specimens were clamped into the load yoke and the test frame. Any combination of bending and torsion could be applied by adjusting the amplitude and phase of the two independent, hydraulic actuators. Tests on the tube-to-plate weldments were carried out under load control using

Table 1 Residual stress distribution on or near the outer surface of the tube in as-welded tube-to-plate specimens

Location distance from weld toe (mm) (See Fig. 2)	Depth (*mm*)	*Measured and calculated residual stress (MPa)*		
		*Longitudinal**	*Tangential**	*Radial†*
weld toe	0	−534	42	0
	0.05	−430	−82	0
	0.13	−272	29	0
	0.25	−328	−102	0
	0.51	−367	79	0
	1.00	−283	36	−1
38	0	−366	−279	0
	0.05	−189	4	0
	0.13	−188	−81	0
	0.25	−185	−144	1
	0.51	−318	−108	2
	1.00	−271	−87	4
76	0	−311	−356	0
	0.05	−236	−56	0
	0.13	−198	−86	0
	0.25	−278	−134	1
	0.51	−347	−29	2
	1.00	−229	−157	4
114	0	−267	−97	0
	0.05	−197	−39	0
	0.13	−188	−138	0
	0.25	−132	−146	1
	0.51	−108	−44	2
	1.00	−118	−33	3

* Measured values.
† Calculated values.

completely-reversed, constant-amplitude bending, combined bending and torsion, and pure torsion load cycles. The fatigue test results are listed in Table 2. The fatigue test data are plotted in the S–N diagrams of Figs 5–7 using several definitions of stress: bending stress (neglecting any torsional stresses), S_a^B, equivalent stress (von Mises criterion $S_a^E = \{(S_a^B)^2 + 3(S_a^T)^2\}^{1/2}$), and maximum principal stress ($S_a^P = S_a^B/2 + \{(S_a^B)^2/4 + (S_a^T)^2\}^{1/2}$). The test data correlate best when plotted against the maximum principal stress, which includes the effect of the torsional shearing stresses.

Shearing stresses reduced the fatigue life of tube-to-plate welds subjected to combined bending and torsion, as had been observed earlier by Munse (1). All specimens failed at the weld toe on the tube except for the pure torsion tests which, for the as-welded weldments (compressive weld toe residuals), did not fail at the weld toe but from small defects on the seamless tubing outer surface. For this reason, the pure torsion results were not plotted in Figs 5–7. Stress relief reduced the fatigue life of specimens because the residual stresses at the

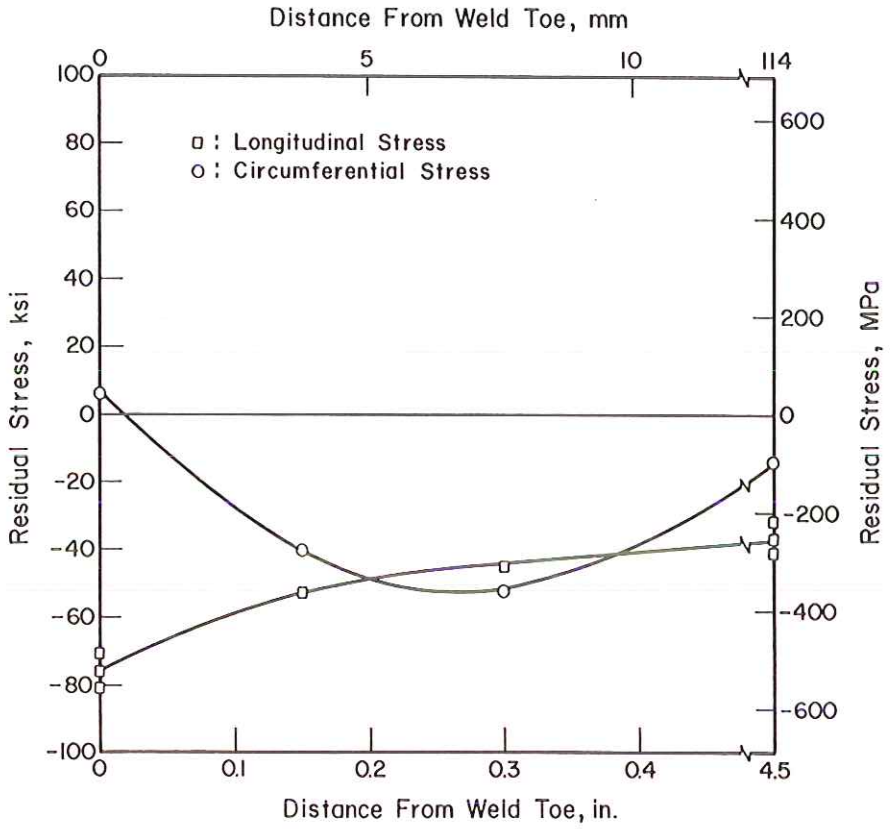

Fig 3 Residual stress distribution on the outer surface of tube-to-plate specimen: see Fig. 2 for definition of coordinates

weld toe were compressive. The fracture surfaces of the welds subjected to combined bending and torsion had a characteristic 'factory-roof' appearance due to multiple crack initiation along the weld toe and a tendency of the initiated cracks to propagate at an angle prior to linking with adjacent initiated cracks.

Crack initiation was monitored using the pulse-echo ultrasonic technique with surface wave transducers, but this method did not give reliable indications of small initiated fatigue cracks. Replicas of the weld toe were taken periodically to establish the presence of an initiated crack. The replica studies indicated that multiple crack initiation occurred at the weld toe and that initiation and early growth were constrained to the line of the weld toe, as had been the experience of Fash (**4**) with notched shafts. Two stress-relieved specimens were removed from the testing apparatus and heat-tinted at lives corresponding to calculated estimates of the fatigue crack initiation lives (N_I).

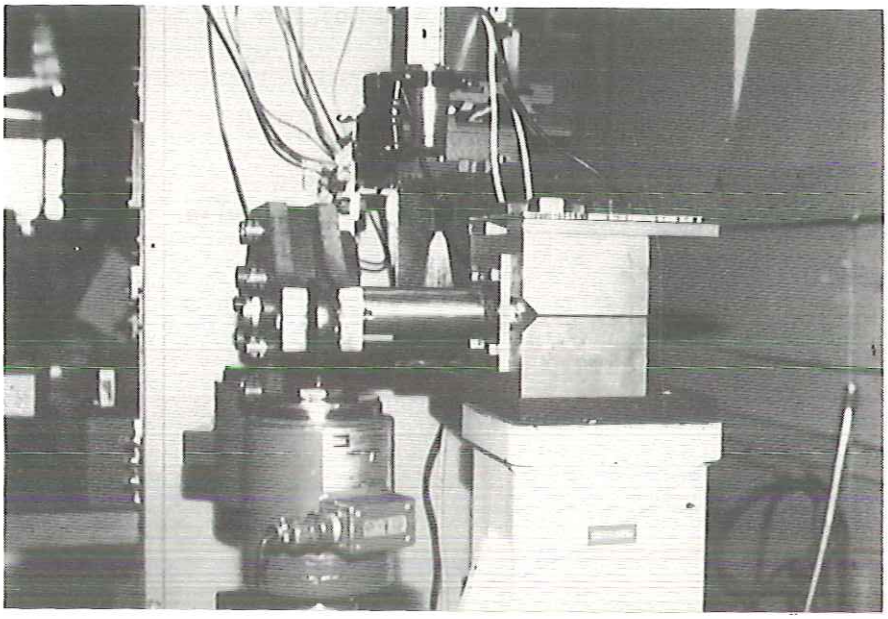

Fig 4 Testing apparatus for welds subjected to combined bending and torsion

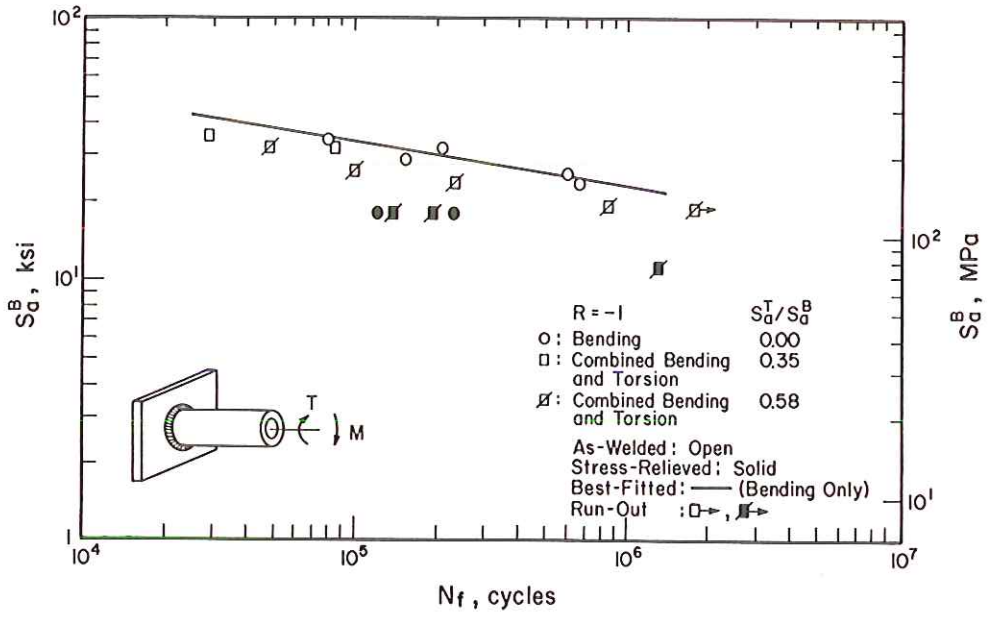

Fig 5 Fatigue life versus bending stress amplitude S_a^B at the weld toe for as-welded tube-to-plate specimens with a stress ratio $R = -1$

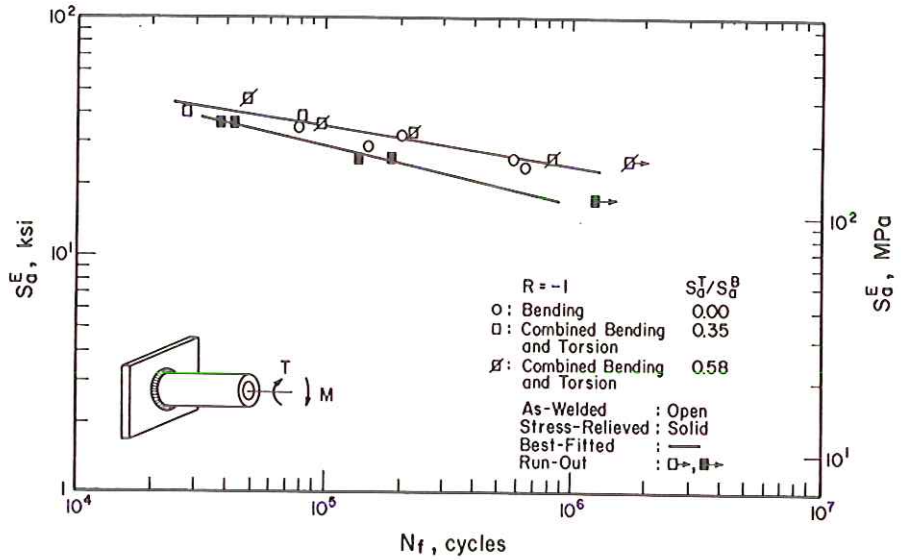

Fig 6 Fatigue life versus equivalent stress amplitude S_a^E at the weld toe (octahedral stress amplitude) for as-welded and stress-relieved tube-to-plate specimens with a stress ratio $R = -1$

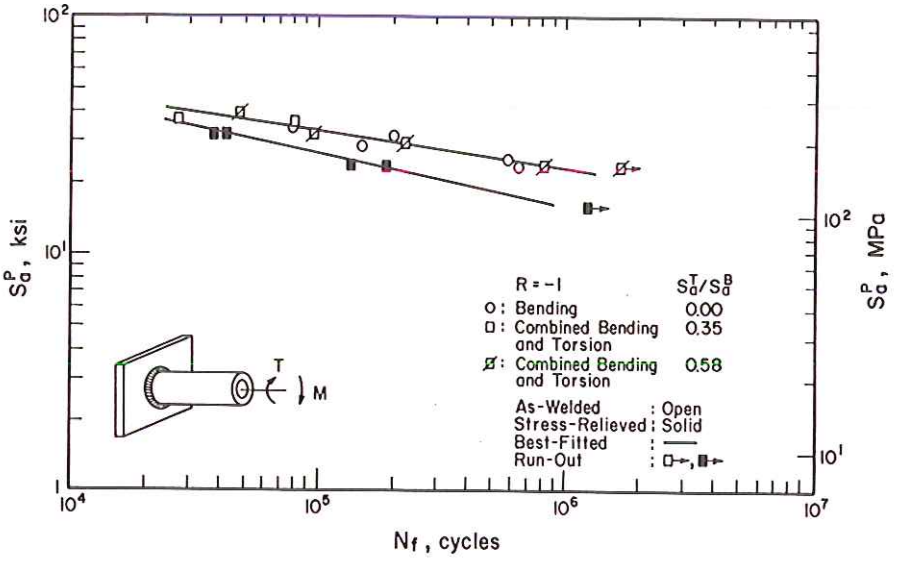

Fig 7 Fatigue life versus maximum principal stress amplitude S_a^P at the weld toe for the welded and stress-relieved tube-to-plate specimens with a stress ratio $R = -1$

Table 2 Fatigue test results for tube-to-plate welds

Welds	*Weld toe bending moment amplitude (Nm)*	*Torsional moment amplitude (Nm)*	*Weld toe normal stresses* S_a^B *(MPa)*	S_a^T *(Mpa)*	S_a^T/S_a^B	*Fatigue life,* N_f*, (cycles)*
As-welded	974	–	230	–	0	76 660
	925	–	218	–	0	198 000
	852	–	201	–	0	145 690
	733	–	173	–	0	560 850
	674	–	159	–	0	624 330
	974	677	230	79	0.34	27 100
	925	1057	218	125	0.57	47 090
	925	704	218	83	0.38	78 620
	733	847	173	100	0.57	93 690
	674	779	159	92	0.57	220 030
	550	637	130	75	0.57	788 370
	550	637	130	75	0.57	>1 641 740
	–	1185	–	140	∞	466 860
	–	1016	–	120	∞	827 560
Stress-relieved	733	847	173	100	0.57	42 440
	550	637	130	75	0.57	132 650
	550	637	130	75	0.57	183 250
	331	383	78	45	0.57	>1 209 700

Finite element studies

The relationships between the remote and the notch-root stresses and strains were studied using elastic–plastic finite element methods. The ABAQUS (**8**) software with three-dimensional, twenty-noded solid elements was used to generate the mesh shown in Fig. 8 which contained 96 elements and 624 nodes. A refined mesh and a notch-root radius of 0.25 mm was established at the weld toe, which value corresponds to the worst-case notch-root conditions (**9**). The stabilized cyclic notch-root material properties used in the finite element calculations were estimated based on hardness measurements and metallography of the weld microstructural zones and on previous studies of the fatigue properties of ASTM A36 weld microstructures (**10**). The material properties of ASTM A36 HAZ used in this study are summarized in Table 3. The elastic stress concentration factors (K_t) for bending and torsion were found to be 4.06 and 1.90, respectively*.

The ABAQUS software has provisions for considering the effects of residual (initial) stresses; however, our experience was that this initial stress condition subroutine would work for tensile but not compressive residual stresses. Consequently, Table 4 lists calculated results only for the stress-relieved test pieces.

* The K_t values are the magnification of the nominal bending and torsional stresses at the weld toe by the discontinuity of the weld toe, i.e. $\sigma_a^B = K_t^B S_a^B$, $\tau_a^T = K_t^T S_a^T$.

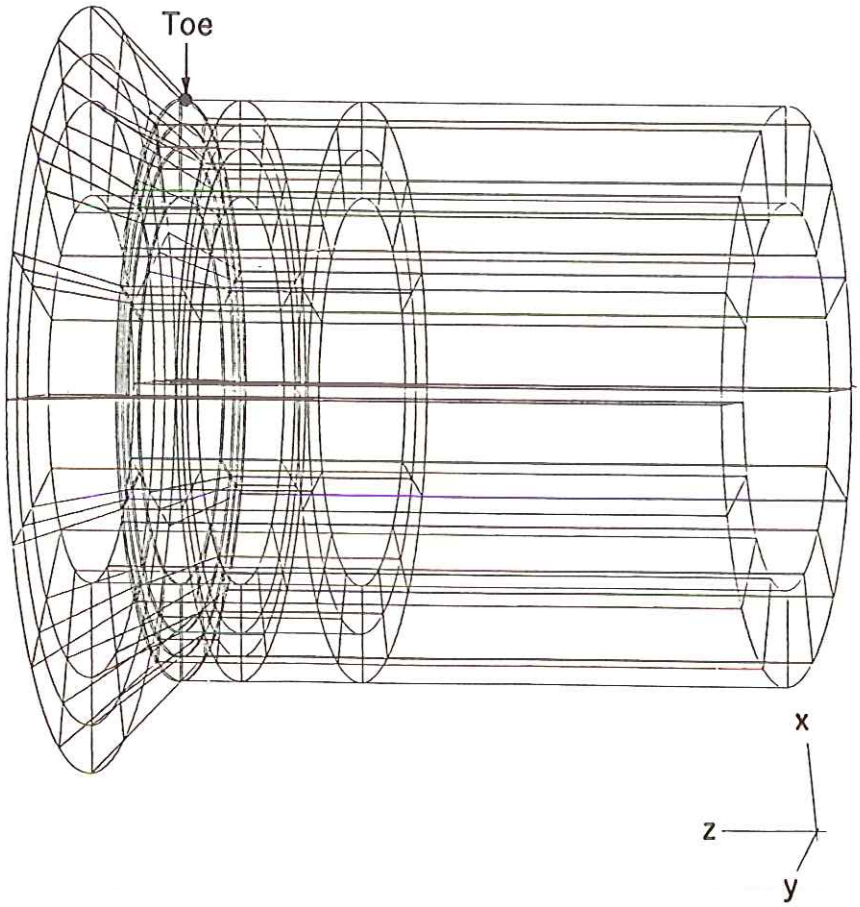

Fig 8 Finite element mesh of tube-to-plate welds (ratio of notch-root element size to notch radius = 1:4). The weld toe of interest is located at the intersection of the cone with the hollow cylinder

Estimates of the fatigue crack initiation life using multiaxial theories

The analytical estimates of the fatigue crack initiation lives listed in Table 5 were obtained using equations (3)–(5) and notch root strains predicted from the remote loading conditions and the results of the FEM analysis summarized in Table 4. The most reliable measurements of initiated crack size were provided by two heat-treated specimens which were heat-tinted at lives corresponding to calculated values of fatigue crack initiation life. These test pieces were subjected to combined bending and torsion ($S_a^T/S_a^B = 0.58$). Although battering of the fracture surfaces by the reversed loadings nearly eradicated the distinction between the heat-tinted fractured and the other fractured regions in the two specimens, crack depths of 1.2 mm and 1.4 mm could be measured at lives of

Table 3 Mechanical properties of ASTM A36 HAZ

Monotonic properties		
Elastic modulus, GPa (ksi)	E	210 (30 400)
Yield strength (0.2%), MPa (ksi)	S_y	565 (82)
Tensile strength, MPa (ksi)	UTS	752 (109)
Reduction in area	%RA	49%
True fracture strength, MPa (ksi)	σ_f	1007 (146)
True fracture ductility	ε_f	0.78
Strength coefficient	K	1103 (106)
Strain hardening exponent	n	0.11
Cyclic properties		
Fatigue ductility coefficient	ε'_f	0.28
Fatigue ductility exponent	c	−0.60
Fatigue strength coefficient, MPa (ksi)	σ'_f	1090 (158)
Fatigue strength exponent	b	−0.091
Cyclic strength coefficient MPa (ksi)	K'	1110 (161)
Cyclic strain hardening exponent	n'	0.15
Cyclic yield strength, MPa (ksi)	S'_y	464 (63)
Propagation properties		
Crack growth coefficient ($R = 0$)	C	6.89×10^{-12}
Crack growth exponent ($R = 0$)	n	3.0
Fracture toughness, MPa$\sqrt{m}$ ($R = 0$)	K_c	85

Table 4 Cyclically stable weld toe strain amplitudes computed by finite element analysis for stress-relieved specimens

Bending (*Nm*)	*Torsion* (*Nm*)	*Micro-strains*, $\mu\varepsilon$*					
		ε_{xx}	ε_{yy}	ε_{zz}	γ_{xy}	γ_{yz}	γ_{xz}
733	847	−390	−1570	1962	−300	−5770	3820
550	637	−45	−530	1371	−408	−1650	1230
331	383	−27	−320	825	−295	−1190	74

* See Fig. 8 for definition of axes: z is parallel to tube length, y is circumferential along the weld toe, and x is normal to the tube surface.

Table 5 Fatigue crack initiation life prediction for stress-relieved specimens

Bending moment amplitude (*Nm*)	*Torsional moment amplitude* (*Nm*)	N_f(*cycles*)	N_I*predicted* (*cycles*)		
			Maximum shear strain	*Lohr–Ellison parameter*	*Kandil–Brown–Miller parameter*
773	847	42 440	1033	1863	1538
550	637	132 650	55 850	60 500	77 000
550	637	183 250	55 850	60 500	77 000
331	383	>1 209 700	1 590 000	2 400 000	3 225 000

1538 and 77 000 cycles. These lives corresponded to the crack initiation lives (N_I) predicted by the Kandil–Brown–Miller parameter and the Coffin–Manson relationship (see equation (5) and Table 5) and accounted for 4 per cent and 50 per cent of the observed total fatigue lives (N_f = 39 000 and 150 000 cycles), respectively. These results are in accord with our general belief (based on experience with other welds subjected to uniaxial cyclic stresses) that crack initiation and early growth become increasingly important and, indeed, dominant at long lives.

Analytical estimates of the total fatigue life using the Basquin equation

If, at long lives, fatigue crack initiation becomes dominant, then estimates of the crack initiation life can be used as approximations to the total fatigue life. The authors have been using the Basquin equation to estimate the fatigue resistance of welds subjected to axial and bending stresses at lives greater than 10^6 cycles (**11**). This approach assumes worst-case notch conditions for the value of the fatigue notch factor, K_f (**11**). These concepts were applied to the tube-to-plate welds of this study as an alternate approach to predicting their total fatigue lives. We assumed that the worst-case notch idea was also valid for welds subjected to torsion and that at long lives the local stress–strain behavior was elastic. The local equivalent stress amplitude predicted by the von Mises criterion (σ_a^E) and the maximum principal stress amplitude (σ_a^P) are given by the expressions below

$$\sigma_a^E = \{(K^B_{f\max} S^B_a)^2 + 3(K^T_{f\max} S^T_a)^2\}^{1/2} \quad (6)$$

$$\sigma_a^P = (K^B_{f\max} S^B_a/2) + \{(K^B_{f\max} S^B_a/2)^2 + (K^T_{f\max} S^T_a)^2\}^{1/2} \quad (7)$$

Table 6 High cycle fatigue life predictions made using the modified Basquin equation

	Weld toe stresses			N_f *predicted (cycles*)*	
Welds	S^B_a *(MPa)*	S^T_a *(MPa)*	N_f *observed (cycles)*	*Equivalent stress*	*Maximum principal stress*
As-welded	216	–	198 000	32 791	32 791
	193	–	145 000	114 663	114 663
	172	–	560 850	409 671	409 671
	159	–	624 330	1 045 475	1 045 475
	159	92	220 030	211 979	360 113
	130	75	788 370	2 042 793	3 467 552
	130	75	>1 641 740	2 042 793	3 467 552
Stress-relieved	130	75	132 650	51 433	87 302
	130	75	183 650	51 433	87 302
	78	45	>1 209 700	15 667 520	26 611 197

* Values predicted using equations (6)–(8) and taking σ'_f = 1090 MPa, $\sigma_r \approx -431$ MPa for the as-welded condition and ≈ -43 MPa for the stress-relieved condition, $b = -0.091$, $K_{f\max} = 2.53$ (bending) and 1.45 (torsion): see Table 3.

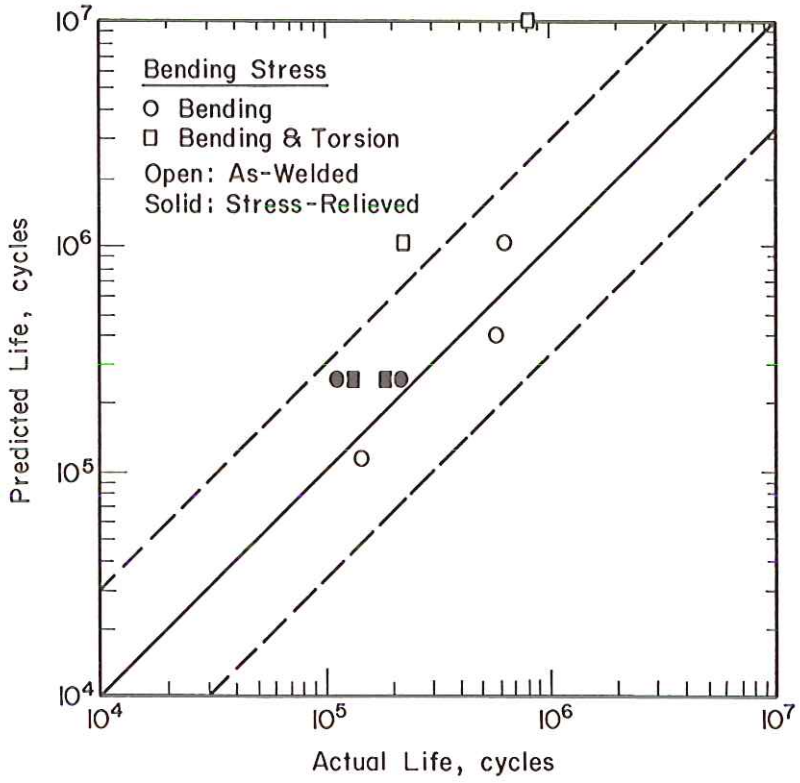

Fig 9 Comparison of actual and predicted fatigue lives using local bending stress σ_a^B and the modified Basquin equation

where the superscripts B and T indicate bending and torsion, respectively. For completely reversed loading, the local mean stress will be equal to the residual stress at the weld toe. While Niku-Lari (**12**) used both Dang Van's criterion and the von Mises criterion to estimate the combined effects of mean and residual stresses in unnotched specimens, it seems most reasonable, for notched specimens such as the welds considered here, to use the component of residual (and mean) stress perpendicular to the weld toe, inasmuch as the initiation and early growth of fatigue cracks was confined to the line of the weld toe despite attempts to depart from this line which gave rise to the factory roof fracture surface appearance mentioned. The modified Basquin equation becomes

$$\sigma_a^E \text{ (or } \sigma^P{}_a) = (\sigma_f' - \sigma_r)(2N_f)^b \tag{8}$$

From the elastic–plastic finite element analyses for the worst-case notch condition (**11**) (notch root radius equal to Peterson's parameter, a), the elastic stress concentration factors for bending and torsion were found to be 4.06 and 1.90, respectively. The corresponding values of the worst-case fatigue notch

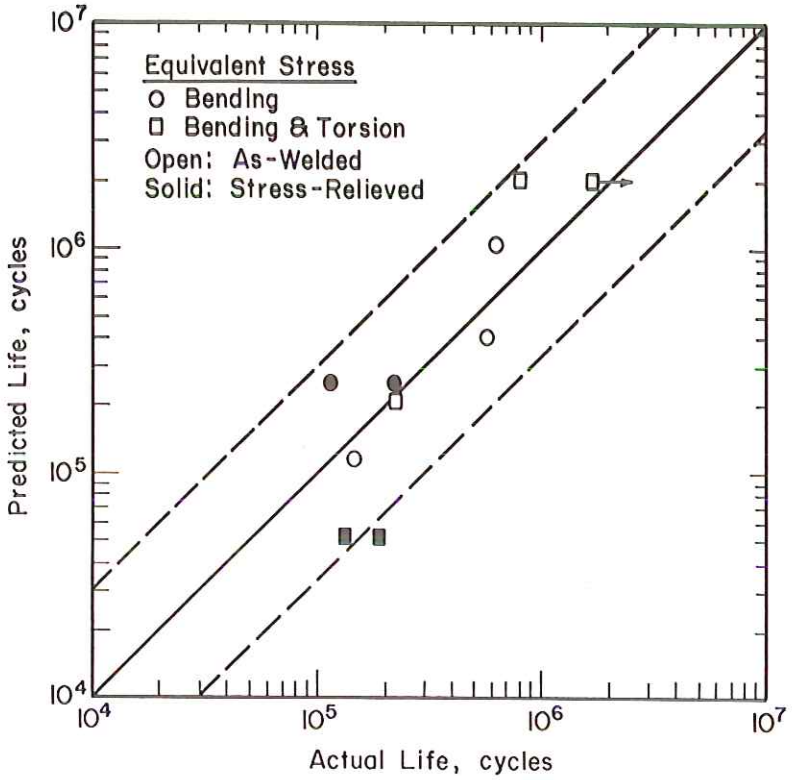

Fig 10 Comparison of actual and predicted fatigue lives using local equivalent stress amplitude σ_a^E (octahedral shearing stress amplitude) and the modified Basquin equation

factor (K_{fmax}) were 2.53 for bending and 1.45 for torsion. The average longitudinal residual stress at a 0.25 mm depth was −431 MPa for the as-welded condition. Ten per cent of this residual stress was assumed to persist after the stress relief treatment (**13**). The fatigue properties of the HAZ were estimated using measured hardness values and the empirical relationships given in (**14**). Total life estimates made using the Basquin equation and the approach outlined above are given in Table 6. Comparisons of the fatigue lives predicted using the Basquin equation approach (equation (8)) and the observed lives are plotted in Figs 9–11. The predictions generally agree with the observed lives within a factor of three except for the comparison based on bending stresses only (Fig. 9).

Summary and conclusions

Although a limited number of tests were performed in this short study, several conclusions can be drawn. The tube-to-plate welds proved to be a successful

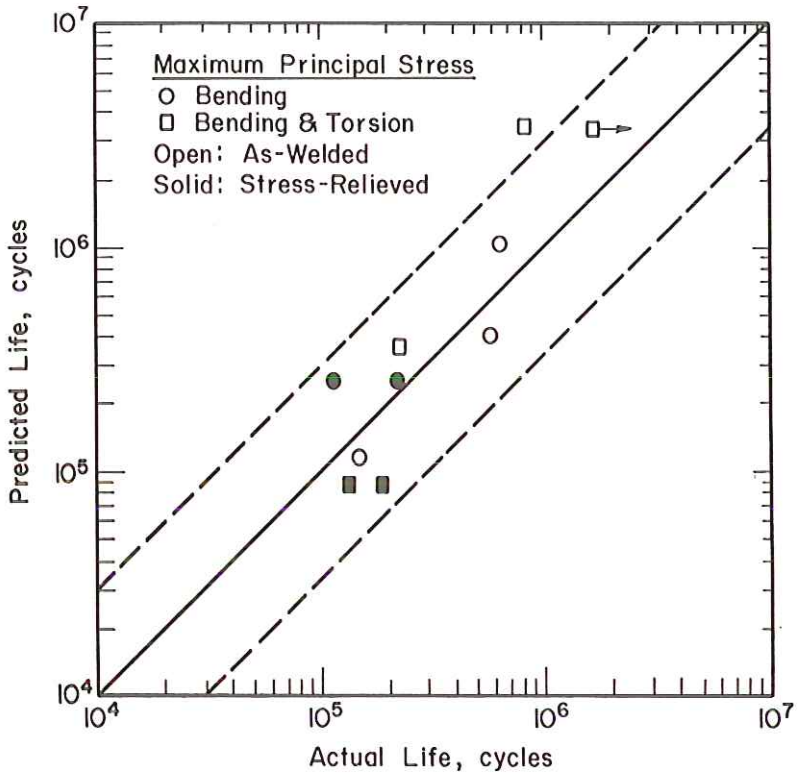

Fig 11 Comparison of actual and predicted fatigue lives using local maximum principal σ_a^P and the modified Basquin equation

geometry for the study of the combined effects of bending and torsion on weldments. The combined bending and torsion loadings studied gave lives about a factor of three less than pure bending stresses, so that multiaxial stress states do influence the fatigue resistance of weldments, despite the two-dimensional nature of the weld-toe notch and its relative insensitivity to pure torsional loading. Residual stresses were found to play an important role in determining the fatigue life period devoted to crack initiation and early growth. The multiaxial fatigue theories of Lohr and Ellison and Kandil, Brown, and Miller both gave reasonable estimates of fatigue crack initiation life when the notch root strains could be determined. For applications involving notches, one must resort to methods such as elastic–plastic finite element analyses to estimate the required notch-root strains. Estimates of initiation life based on Basquin's equation modified for multiaxial stresses gave predictions for long-life fatigue life which were within a factor of three of the observed total lives.

Acknowledgements

This study was supported by the University of Illinois Fracture Control Program which is funded by a consortium of midwest ground vehicle industries. The authors wish to thank Professor Darrel Socie of the Department of Mechanical Engineering and Dr James W. Fash for the use of their test apparatus and their kind assistance in setting up the experiments described.

References

(1) MUNSE, W. H. and STALLMEYER, J. E. (1962) *Fatigue in welded beams and girders*, Bulletin 315, Highway Research Board, Washington, DC.

(2) LOHR, R. D. and ELLISON, E. G. (1980) A simple theory for low cycle multiaxial fatigue, *Fatigue Engng Mater. Structure*, **3**, 1–17.

(3) KANDIL, F. A., BROWN, M. W., and MILLER, K. J. (1982) Biaxial low-cycle fatigue fracture of 316 stainless steel at elevated temperatures, *Book 280*, The Metals Society, London, pp. 203–210.

(4) FASH, J. W. (1985) An evaluation of damage development during multiaxial fatigue of smooth and notched specimens, University of Illinois, Materials Engineering Report No. 123.

(5) FASH, J. W., SOCIE, D. F., and McDOWELL, D. L. (1982) Fatigue life estimates for a simple notched component under biaxial loading, Department of Mechanical and Industrial Engineering, University of Illinois at Urbana-Champaign.

(6) SOCIE, D. F., WAILL, L. A., and DITTMER, D. F. (1983) Biaxial fatigue of Inconel 718 including mean stress effects, Department of Mechanical and Industrial Engineering, University of Illinois at Urbana-Champaign.

(7) LEGGATT, R. H. (1984) Residual stresses at girth welds in pipes, *Welding in energy-related projects*, (Welding Institute of Canada) Pergamon Press, Oxford.

(8) HIBBITT, KARLSSON, and SORENSON, INC., Providence, RI, 1980.

(9) LAWRENCE, F. V., MATTOS, R. J., HIGASHIDA, Y., and BURK, J. D. (1978) *Estimation of fatigue crack initiation life of weld, ASTM STP 648*, American Society of Testing and Materials, Philadelphia, PA, p. 420.

(10) HIGASHIDA, Y. and LAWRENCE, F. V. (1976) Strain controlled fatigue behavior of weld metal and heat-affected base metal in A36 and A514 steel welds, FCP Report No. 22, College of Engineering, University of Illinois at Urbana-Champaign.

(11) YUNG, J.-Y. and LAWRENCE, F. V., Jr (1985) Analytical and graphical aids for the fatigue design of weldments, *Fatigue Fracture Engng Mater. Structures*, **8**, 223–241.

(12) NIKU-LARI, A. (1983) Influence of residual stresses introduced by shot peening upon the fatigue life of materials, *Expl Techniques*, March, 21–25.

(13) *Fundamentals of Welding, Welding Handbook Vol. 1*, (Seventh Edition) 1976, American Welding Society, pp. 271–272.

(14) McMAHON, J. C. and LAWRENCE, F. V. (1984) Predicting fatigue properties through hardness measurements, FCP Report No. 105, College of Engineering, University of Illinois at Urbana-Champaign.